

# What Is the Solvation Number of Na<sup>+</sup> in Ammonia? An Ab Initio QM/MM Molecular Dynamics Study

Teerakiat Kerdcharoen\*

Department of Physics, Faculty of Science, Mahidol University, Bangkok 10400, Thailand

Bernd M. Rode

Department of Theoretical Chemistry, Institute of General, Inorganic and Theoretical Chemistry, University of Innsbruck, A-6020, Innsbruck, Austria

Received: December 13, 1999; In Final Form: March 29, 2000

An ab initio molecular dynamics simulation based on combined quantum mechanical and molecular mechanical (QM/MM) potential was performed for Na<sup>+</sup> in liquid ammonia. With this approach, many-body interactions that are very significant in determining the solvation number are modeled accurately by quantum mechanics. The method appears to resolve the discrepancy between many simulations that have predicted solvation numbers between 5 and 9. Although the solvation number of 5 obtained from our QM/MM simulation has not yet been confirmed by the experimental data, a detailed analysis of the simulation results together with a comparison of previous studies on known systems justifies this prediction.

## 1. Introduction

In recent years, molecular simulations using molecular dynamics<sup>1</sup> and Monte Carlo<sup>2</sup> methods have become the principal and common tools for scientists to study phenomena at molecular level. Continuous improvements in both hardware technology and computational techniques have helped to expand the application of these tools to a wider spectrum of scientific disciplines ranging from physics and chemistry to biological sciences.<sup>3–5</sup> Despite the success of these tools in describing numerous chemical systems, researchers still suffer from the reality of the “potential energy model”, used as input of the simulations.<sup>6–8</sup> Most potential energy models assume that the total energy of the system is simply the summation of the interactions between pairs of particles, thus neglecting higher order terms. The reason is the complicated orientation dependence of molecular systems that makes the accurate construction of even three-body potentials very expensive. The construction of three-body energy surfaces may require many thousands of SCF energy points to include all important regions. Moreover, due to the asymptotic behavior of the three-body potential, fitting of ab initio energies to an analytical formula is sometimes a difficult trial-and-error task. Accordingly, most three-body potential functions are tailored by some means, for instance, by removing some energy points and weighting more energy points in some important regions to obtain a good fit and by neglecting some configurations on the assumption that they rarely happen in the simulation.<sup>9,10</sup>

The difficulty in describing the potential energy by analytical functions calls for ab initio molecular dynamics that calculate interactions between particles from the first principles within the simulation. This approach allows more accurate interaction potentials to be calculated from the instantaneous configurations by ab initio methods whereby many-body effects are included up to the degree determined by the number of particles included

in the QM region. A quantum mechanical treatment of the entire system is still not feasible at present. Consequently, a hybrid approach such as the combined quantum-mechanical/molecular-mechanical (QM/MM) method was proposed to solve this problem.<sup>11,12</sup> The key concept is that quantum mechanical treatment is undertaken to a full extent for a selected, chemically relevant region, and the rest of the system is left to be treated by molecular mechanics.

Although most early applications of the QM/MM method have used only semiempirical schemes,<sup>13–15</sup> recent advances in computer technology allow a full ab initio treatment of the QM region. This is an important advantage because more complex problems, e.g., ion solvation, require more accurate methods than semiempirical schemes as demonstrated in our previous simulations of Li<sup>+</sup> in liquid ammonia.<sup>16</sup> In the meantime, numerous solvated ions have been investigated by ab initio QM/MM simulations, mostly hydrated ions such as Li<sup>+</sup>, Na<sup>+</sup>, K<sup>+</sup> and Ca<sup>2+</sup>.<sup>17–19</sup> In the present work, Na<sup>+</sup> in liquid ammonia is studied by an ab initio Hartree–Fock QM/MM method. The investigation of this system by a QM/MM method is quite challenging because the solvation number for this system is very sensitive to the quality of the potential energy model. Molecular dynamics simulation using ab initio pair potential based on primitive Gaussian basis sets gave a solvation number of 8.<sup>20</sup> Subsequent Monte Carlo simulations using improved ab initio pair potentials based on DZP basis sets lead to the solvation number 9.<sup>9</sup> Inclusion of three-body functions into the potential model reduces this number to 8.<sup>9</sup> With regard to the experiences with Li<sup>+</sup> in liquid ammonia, this number still appears to be too high. Considering Na<sup>+</sup> in water, replacement of the pair potential by the QM/MM potential removes one water molecule from the first hydration shell, thereby leading to the hydration number of 5.6.<sup>18</sup> Consequently, it seems plausible that more than one ammonia molecule could be removed from the first solvation shell of Na<sup>+</sup> in ammonia if a QM/MM potential model were used, especially since many-body interactions in

\* To whom correspondence should be addressed. E-mail: sctkc@mahidol.ac.th.

Na<sup>+</sup>/ammonia are 2 times higher than in the aqueous system.<sup>21</sup> Furthermore, a Monte Carlo simulation by Marchi et al.<sup>22</sup> gave a surprisingly small solvation number of 5. In this work, a classical pair potential augmented by implicit ion–dipole polarization terms averaging some of the many-body interactions was used. Hence, one could expect that inclusion of higher many-body interactions by ab initio QM/MM treatment of the whole first solvation shell would eliminate discrepancies among previous studies, thus leading to a more or less final result.

## 2. Models and Methods

**2.1 QM/MM terms and Definitions.** Interactions within a QM/MM system consist of three parts: (1) the QM part, (2) the MM part, and (3) the interaction between QM and MM regions. The Hamiltonian of this system, modified from Ref.,<sup>23</sup> can be written as

$$H = H_{QM} + H_{MM} + H_{QM/MM} \quad (1)$$

where

$$H_{QM} = \sum_I^{QM} \frac{P_I^2}{2m_I} + \sum_{I>J}^{QM} \frac{Z_I Z_J}{R_{IJ}} + \langle \Psi | \hat{H}^{el} | \Psi \rangle \quad (2)$$

$$H_{MM} = \sum_A^{MM} \frac{P_A^2}{2m_A} + V_{MM} \quad (3)$$

and

$$H_{QM/MM} = \sum_I^{QM} \sum_A^{MM} \frac{Z_I Q_A}{R_{IA}} - \sum_i^{QM} \sum_{MM}^A \left\langle \Psi \left| \frac{Q_A}{r_{iA}} \right| \Psi \right\rangle + V_{IA}^{nc} \quad (4)$$

where *I* and *A* denote the atoms of the QM and MM molecules, respectively. The first term in eq 2 represents the kinetic energy, whereas the second and the third describe internuclear repulsions and electronic potential in the QM region, respectively. The electronic Hamiltonian operator in our work is defined for the isolated QM region only, thus excluding electron polarization effects induced by the surrounding MM molecules. *H<sub>MM</sub>* comprises kinetic and potential energies for which the potential function *V<sub>MM</sub>* is described in Section 2.3.

The coupling between QM and MM regions, eq 4, is more complex. The first term describes electrostatic interactions between nuclear charges of atoms in QM molecules and partial atomic charges of the MM atoms. The second term represents electrostatic interactions between electrons of the QM molecules and partial atomic charges located on the MM atoms. *V<sub>IA</sub><sup>nc</sup>* is the non-Coulombic part of *V<sub>MM</sub>*. Equation 4 can be approximated by

$$H_{QM/MM} \approx \sum_I^{QM} \sum_A^{MM} \frac{Z_I Q_A}{R_{IA}} - \sum_I^{QM} \sum_A^{MM} \frac{Q_I Q_A}{R_{IA}} + V_{IA}^{nc} \quad (5)$$

where *Q<sub>I</sub>* is the effective electronic charge on atom *I* that after averaging over nuclear charge leads to

$$H_{QM/MM} = V_{QM/MM} = \sum_I^{QM} \sum_A^{MM} \frac{Q_I Q_A}{R_{IA}} + V_{IA}^{nc} \quad (6)$$

The *V<sub>QM/MM</sub>* of eq 6 is used in our simulation and is described in Section 2.4.

**2.2 QM potential model.** The first QM/MM scheme for ion solvation defines the QM part as a sphere centered on the ion of interest.<sup>24</sup> In that scheme, it was seen that the suitable size of a spherical QM region may be obtained by a compromise between accuracy and computing time requirement through multiple trial QM/MM simulations. In practice, the diameter of the QM sphere can be selected in such a way that the “chemically relevant” area is totally included, e.g., in the case of solvated ions the first solvation shell whose size can be evaluated by classical MM simulations as performed in all subsequent simulations.<sup>16–19</sup>

However, in the present work, we have extended the spherical QM region even beyond this first solvation shell. Although the time consumption thus increases considerably from the usual 4–5 months to approximately 1 year on a fast workstation (SGI R10000 processor), this extension gives the benefit that the solvation structure up to the second shell can be studied. In addition to that, the first solvation shell itself can be better described since the electronic Hamiltonian operator in eq 2 is improved by the inclusion of electron polarization effects from the outer sphere influencing the first solvation shell.

The QM sphere is modeled by the Hartree–Fock theory based on the effective core potential (ECP) basis functions.<sup>25</sup> The selection of this basis set is consistent with the earlier finding<sup>19</sup> that an ECP that employs extended functions to describe the valence electrons, i.e., double- $\zeta$ , is more reliable than a small all-electron basis set such as STO-3G. In that study, STO-3G overestimates the number of water molecules in the first solvation shell of Ca<sup>2+</sup> from 8.3 to 10. Further analyses of solvation structure and dynamics also show that a larger basis set is necessary for accurate description of intermolecular interactions in the QM region. However, inclusion of a standard-sized all-electron basis set, i.e., 6-31G or DZP, especially with a rather large QM region as in our case, is still beyond current computing capacity. Therefore, a compromise must be made and an ECP basis set that has good quality of basis functions on the valence electrons can be a good choice, as demonstrated in the previous works.<sup>16–19</sup>

Forces on the QM particles can be computed from analytical gradients.<sup>26</sup> To allow exchange of particles between the QM sphere and the MM region, forces must be smoothed at the boundary by applying a suitable function.<sup>27</sup> Thus the force on a particle in the system is defined as

$$f_i = S_m(r_i) f_{QM} + (1 - S_m(r)) f_{MM} \quad (7)$$

where

$$S_m(r) = 1 \text{ for } r \leq r_1$$

$$S_m(r) = \frac{(r_0^2 - r^2)^2 (r_0^2 + 2r^2 - 3r_1^2)}{(r_0^2 - r_1^2)^3} \text{ for } r_1 < r \leq r_0$$

$$S_m(r) = 0 \text{ for } r_0 < r$$

The QM sphere is selected to have a diameter of 10 Å, which is sufficiently large to include the first and a part of the second solvation shell accommodating around 16 solvent molecules. An interval of 0.2 Å applied for the smoothing function led to the values of 5.0 and 4.8 Å for *r<sub>0</sub>* and *r<sub>1</sub>*, respectively.

**2.3 MM potential model.** Because the ammonia molecules in our study are flexible, it is necessary to have an intramolecular potential for solvent molecules in the MM region. No such

**TABLE 1: Optimized Parameters for the Na<sup>+</sup>-Ammonia Intermolecular Potential**

|                    |     |           |                                       |
|--------------------|-----|-----------|---------------------------------------|
| Na <sup>+</sup> -N | a = | -1367.661 | kcal mol <sup>-1</sup> Å <sup>4</sup> |
|                    | b = | 1598.529  | kcal mol <sup>-1</sup> Å <sup>6</sup> |
|                    | c = | 20122.26  | kcal mol <sup>-1</sup>                |
|                    | d = | 2.908240  | Å <sup>-1</sup>                       |
| Na <sup>+</sup> -H | a = | 22.64286  | kcal mol <sup>-1</sup> Å <sup>4</sup> |
|                    | b = | 97.03496  | kcal mol <sup>-1</sup> Å <sup>6</sup> |
|                    | c = | 18.66449  | kcal mol <sup>-1</sup>                |
|                    | d = | 0.7505583 | Å <sup>-1</sup>                       |

definition is needed for the QM molecules since in the QM region all atoms move freely on the Born–Oppenheimer energy surface. The intramolecular and intermolecular potentials for MM ammonia molecules were taken from the literature.<sup>28</sup> The intramolecular potential of ammonia is based on spectroscopic data by Spirko<sup>29</sup> whereas the intermolecular potential was constructed by ab initio methods.<sup>28</sup> These potentials have been tested in many simulations<sup>8–10,20,30–34</sup> and proved reliable and transferable up to supercritical conditions.<sup>34</sup> The MM intermolecular potential for ammonia is atom–atom based and takes the following forms, whose parameters are given in Table 1 of ref 28,

$$V_{MM}(N-N) = \sum_A^{MM} \sum_B^{MM} \left( \frac{a_{NN}}{R_{AB}^{12}} - \frac{b_{NN}}{R_{AB}^6} + \frac{Q_N Q_N}{R_{AB}} \right) \quad (8)$$

$$V_{MM}(H-H) = \sum_A^{MM} \sum_B^{MM} \left( a_{HH} e^{-b_{HH}r} + \frac{Q_H Q_H}{R_{AB}} \right) \quad (9)$$

$$V_{MM}(N-H) = \sum_A^{MM} \sum_B^{MM} \left( a_{NH} (e^{-b_{NH}(R_{AB}-2.4)} - 2e^{-c_{NH}(R_{AB}-2.4)}) + \frac{Q_N Q_H}{R_{AB}} \right) \quad (10)$$

For Na<sup>+</sup>-ammonia, several intermolecular potentials are available from literature,<sup>9,20,22</sup> but we have constructed our own model to demonstrate the dependency of the solvation number on the potential energy model. This model potential is constructed by fitting 600 SCF interaction energies based on the 6-311G++(d,p) basis to an analytical function,

$$V_{MM}(Na^+ - N) = \sum_A^{MM} \sum_B^{MM} \left( \frac{a_{Na^+N}}{R_{AB}^4} + \frac{b_{Na^+N}}{R_{AB}^6} + c_{Na^+N} e^{-d_{Na^+N} R_{AB}} + \frac{Q_{Na^+} Q_N}{R_{AB}} \right) \quad (11)$$

$$V_{MM}(Na^+ - H) = \sum_A^{MM} \sum_B^{MM} \left( \frac{a_{Na^+H}}{R_{AB}^4} + \frac{b_{Na^+H}}{R_{AB}^6} + c_{Na^+H} e^{-d_{Na^+H} R_{AB}} + \frac{Q_{Na^+} Q_H}{R_{AB}} \right) \quad (12)$$

$Q_{Na^+}$  is assumed to be 1.  $Q_N$  and  $Q_H$  obtained from a SCF Mulliken population analysis based on 6-311G++(d,p) using ammonia's experimental geometry are -0.8022 and 0.2674, respectively. The parameters  $a$ ,  $b$ ,  $c$ , and  $d$  in eq 11 and 12 are listed in Table 1. The quality of the fit is demonstrated in Figure 1 by comparing calculated SCF energies with the fitted energies.

**2.4 QM/MM Potential Model.** From eq 6 the QM/MM potential consists of the Coulombic interactions between the net atomic charges of the QM and MM particles and the non-Coulombic part of the MM potential function. These QM/MM potentials consequently take similar forms to eqs 8 – 12. For

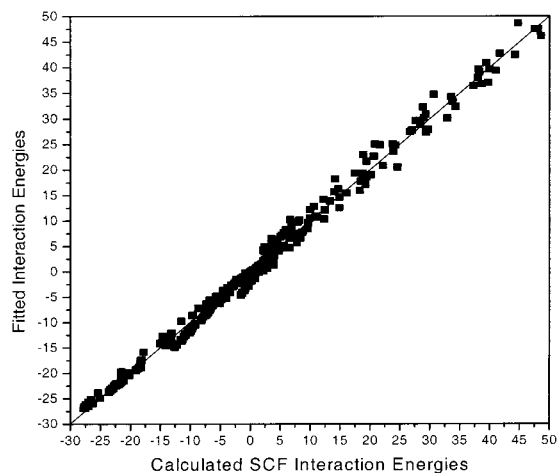


**Figure 1.** Comparison of calculated SCF interaction energies and fitted energies. Energies are given in kcal/mol, Standard deviation from the fit is 1.3 kcal/mol

instance, the QM/MM potential between nitrogen of QM ammonia and nitrogen of MM ammonia reads,

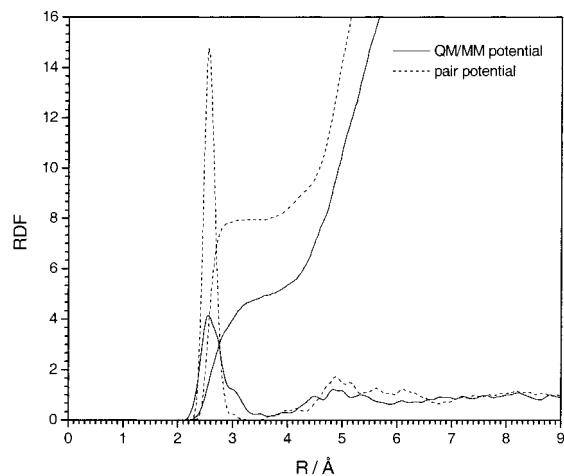
$$V_{QM/MM}(N-N) = \sum_I^{QM} \sum_I^{MM} \frac{Q_N Q_N}{R_{IA}} + V_{IA}^{nc} \\ = \sum_I^{QM} \sum_A^{MM} \frac{Q_N Q_N}{R_{IA}} + \sum_I^{QM} \sum_A^{MM} \left( \frac{a_{NN}}{R_{IA}^{12}} - \frac{b_{NN}}{R_{IA}^6} \right) \quad (13)$$

The QM/MM potentials for other interaction pairs can be constructed in the same way as in eq 13.

**2.5 Simulation Details.** All simulations were performed in the NVT ensemble at 235 K with a time step of 0.2 fs so that fast motion of hydrogen atoms could be described accurately. A periodic cube of length 20.66 Å containing 1 Na<sup>+</sup> and 215 ammonia molecules was chosen, corresponding to the experimental density of liquid ammonia at atmospheric pressure. The potential and forces are smoothed by using a shifted force algorithm and zeroed out at the half-box length.<sup>28</sup> Since the simulated cube is not a neutrally charged system, we employed a reaction field method<sup>35</sup> to handle long-range electrostatic potentials and forces. The simulation started from a randomized configuration and was equilibrated for 30,000 time steps. The simulation was continued for 60,000 time steps to collect configurations every 20th step. For these runs only MM potentials were used, and they will therefore be referred to as the “pair potential simulation”. After that, the QM potential was turned on. The corresponding QM/MM simulation then started from the last configuration, with a reequilibration for 10,000 time steps, after which the simulation was continued for another 10,000 time steps to collect samples every 5th step. Although nowadays a classical simulation of ionic solutions can be extended to several hundred pico-seconds ps, even the 2 ps interval of our QM/MM run approaches the limits of high-speed computing capacity because the QM/MM simulation requires about 15–20 min for a single step on a SGI Power Challenge R10000, which means more than 200 days of computing time for the whole simulation. It has been shown earlier that 2 ps can be sufficient for the analysis of solution structure and some associated dynamics in the simulations of diluted solutions of Be<sup>2+</sup>, Ca<sup>2+</sup>, Li<sup>+</sup>, Na<sup>+</sup>, and K<sup>+</sup> in water<sup>17–19,36</sup> and Li<sup>+</sup> and Na<sup>+</sup> in ammonia.<sup>16,20,28</sup> In an ab initio molecular dynamics simulation

**TABLE 2: Comparison of Solvation Parameters for Na<sup>+</sup>**

| system                   | $r_{\max}$ | RDF( $r_{\max}$ ) | $r_{\min}$ | solvation no.<br>(first shell) | T (K) | ion/solvent | method         | reference |
|--------------------------|------------|-------------------|------------|--------------------------------|-------|-------------|----------------|-----------|
| Na <sup>+</sup> /ammonia | 2.55       | 14.8              | 3.3        | 8                              | 235   | 1/215       | MD (2-body)    | this work |
| Na <sup>+</sup> /ammonia | 2.55       | 4.4               | 3.7        | 5                              | 235   | 1/215       | MD (QM/MM)     | this work |
| Na <sup>+</sup> /ammonia | 2.49       | 16.6              | 3.2        | 8                              | 235   | 1/215       | MD (2-body)    | 20        |
| Na <sup>+</sup> /ammonia | 2.42       | 14.6              | 3.2        | 7                              | 266   | 1/215       | MD (2-body)    | 20        |
| Na <sup>+</sup> /ammonia | 2.68       | 11.6              | 3.6        | 9                              | 277   | 1/201       | MC (2-body)    | 9         |
| Na <sup>+</sup> /ammonia | 2.68       | 10.0              | 3.5        | 8                              | 277   | 1/201       | MC (3-body)    | 9         |
| Na <sup>+</sup> /ammonia | 2.25       | 9.5               | 3.0        | 5                              | 260   | 1/250       | MC (empirical) | 22        |
| Na <sup>+</sup> /water   | 2.36       | 8.1               | 3.0        | 6.5                            | 298   | 1/199       | MD (2-body)    | 18        |
| Na <sup>+</sup> /water   | 2.33       | 5.5               | 2.9        | 5.6                            | 298   | 1/199       | MD (QM/MM)     | 18        |
| Na <sup>+</sup> /water   | 2.45       |                   | 3.5        | 6.6                            | 298   | 1/215       | MD (2-body)    | 39        |
| NaNO <sub>3</sub> (aq)   | 2.44       |                   |            | 6                              |       | 6.0 M       | X-ray          | 40        |
| NaNO <sub>3</sub> (aq)   | 2.40       |                   |            | 4.9                            |       | 3.1 M       | X-ray          | 41        |

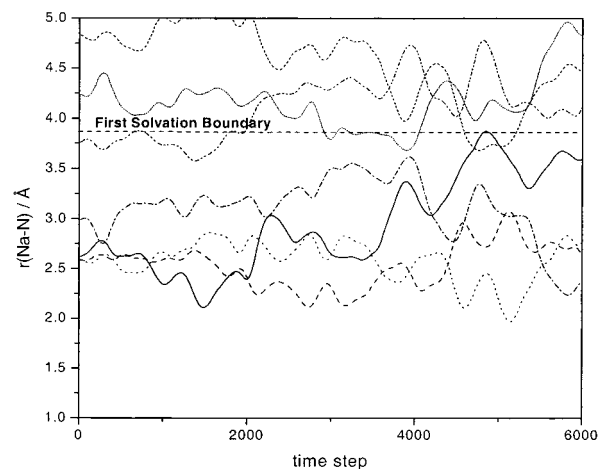
**Figure 2.** Na–N radial distribution function and its running integration numbers.

of aqueous Be<sup>2+</sup> by Parrinello et al.,<sup>36</sup> it was observed that two water molecules escape from the first solvation shell within only 0.25 ps after ab initio potentials are switched on from a classical simulation, thus leading to the coordination number of 4, which is maintained for the total simulation length of 1 ps. In the present work, QM/MM simulation also followed from a classical simulation that has a starting coordination number of 8. Within 0.5 ps, three ammonia molecules were observed to leave the solvation shell. However, calculation of some sensitive dynamical properties such as self-diffusion coefficient require a simulation length up to 100 ps and this is beyond the scope of the present study.<sup>37,38</sup>

### 3. Results and Discussion

Figure 1 demonstrates the quality of fitting the analytical pair potential functions of eqs 11 and 12 to 600 calculated ab initio interaction energies. A good agreement between ab initio interaction energies and fitted values, within both attractive and repulsive regions of the interaction energies, can be seen from points located close to the diagonal line. The global energy minimum for the Na<sup>+</sup>–ammonia complex has the Na<sup>+</sup>–N distance of 2.38 Å, which corresponds to the interaction energy of –27.81 kcal/mol. Although this optimal Na<sup>+</sup>–N distance is equivalent to that obtained by Hannongbua,<sup>9</sup> where Dunning’s DZP basis set was used, our potential model leads to a slightly smaller stabilization.

The Na<sup>+</sup>–N radial distribution functions (RDF) and their running integration numbers obtained from pair potential and QM/MM simulations are presented in Figure 2. To demonstrate the sensitivity of solvation structure on the potential model, a comparison between characteristics of the RDFs obtained from

**Figure 3.** Time evolution of distances between Na<sup>+</sup> and nitrogen of ammonia molecules. The plot includes only ammonia molecules that are involved with the first solvation shell, i.e., locating inside, entering into, or exiting from. In this plot, the seven ammonia molecules involved are depicted with different type of lines.

various simulations is given in Table 2. The Na<sup>+</sup>–N RDF of the pair potential simulation exhibits a sharp, narrow, and well-separated peak located between 2.3 and 3.3 Å, which leads to a solvation number of 8. The QM/MM method depicts a less rigid solvation structure, as can be observed from the lower, broader, and less symmetric 1st shell peak, which corresponds to an average solvation number of 5. In contrast to the pair potential simulation, the first solvation shell of the QM/MM simulation is not clearly separated from the second one, which indicates that an exchange of solvent molecules between both shells takes place much more easily than expected from the “classical” simulation. Motions of solvent molecules that enter into and exit from the first solvation shell were monitored in the course of the simulation, and the ion–nitrogen distances with the time evolution for these solvent molecules are plotted in Figure 3. This plot excludes solvent molecules that have moved close to the first solvation shell but never entered it. It can be seen that during a period of 1.2 ps solvent molecules cross the boundary 13 times in both directions. In fact, only 4 solvent molecules restrict their motions to an area within the first solvation shell, whereas one solvent molecule is exchanged between the first and second shells. This behavior is reflected by a shoulder in the first Na<sup>+</sup>–N RDF peak. Because of this solvent exchange, the first solvation shell becomes larger than that obtained from the classical simulation. This result also indicates that for discussion of ligand exchange mechanisms of weak complexes, a basis of a highly accurate simulation is needed to predict the microspecies present in solution because the simultaneous presence of more than one species will have a



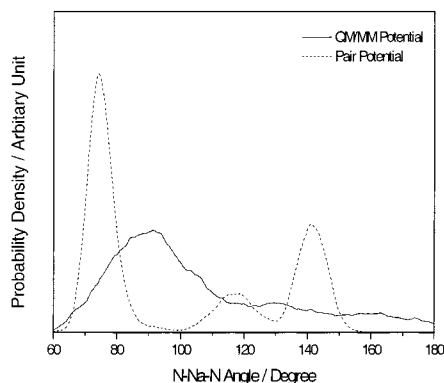


**Figure 4.** N-Na-N angular distribution for the first solvation shell.

considerable influence on the reaction pathways for such exchange processes.

As a consequence of the absence of experimental data for Na<sup>+</sup>-ammonia solutions, there is no way to ascertain whether the solvation number obtained from the QM/MM simulation is the “true” value. However, the comparison of the results obtained by this method for other similar systems can help in evaluating its reliability: A previous QM/MM simulation of Li<sup>+</sup> in ammonia solution gave a coordination number of 4, in line with neutron diffraction experiments, while pair and three-body potential simulations yielded an octahedral solvation structure.<sup>16</sup> It has been shown that many-body interactions in Li(NH<sub>3</sub>)<sub>6</sub><sup>+</sup> are as large as 26% and still amount to 21% in Na(NH<sub>3</sub>)<sub>6</sub><sup>+</sup>.<sup>21</sup> This is sufficiently high to effect the solvation number. Therefore, we believe that the solvation number of 5 obtained in our QM/MM simulation should be correct. The discrepancy between our QM/MM and three-body simulation results may be attributed to the incompleteness of the three-body function itself and the inclusion of higher contributions (up to the order of 15) in the QM/MM potential.

The orientation of solvent molecules around the ion in the first solvation shell is demonstrated in terms of angular N-Na<sup>+</sup>-N distribution as shown in Figure 4. The distribution pattern in the case of pair potential simulation is similar to that found for Mg<sup>2+</sup> in ammonia<sup>9</sup> and Ca<sup>2+</sup> in ammonia,<sup>30</sup> for which the solvation numbers are 8 as well. Therefore, a distorted cubic structure has been assigned to these solvation shells. For the solvation number of 5, one could assume two main structures, namely a trigonal bipyramid and a square pyramid. The bipyramidal structure is characterized by N-Na<sup>+</sup>-N angles of 90, 120, and 180 degrees with a probability ratio of 6:3:1. The square pyramid would provide angles of 90 and 180 degrees with a probability ratio of 8:2. As seen from Figure 4, a well-pronounced peak around 90 degrees emerges with a relatively high probability ratio, which indicates that a distorted square pyramidal solvation shell would be more likely than the bipyramidal one whose structure has lower probability for the angle of 90 degrees. Within this context one should also consider the small shoulder observed in the Na<sup>+</sup>-N RDF between 3 and 3.7 Å. Without this shoulder, a near-tetrahedral structure could have been obtained (as seen from the running integration number of 4 up to this distance). The close approach of a further solvent molecule into this structure could lead to a rather square pyramidal or planar arrangement of the first four solvent molecules plus an additional elongated Na<sup>+</sup>-N bond to the incoming solvent molecule. The resulting structure would allow an easier solvent exchange. Figure 3 confirms that it is always the solvent molecule with elongated Na<sup>+</sup>-N distance, i.e., between 3 and 3.7 Å, that is exchanged with another one from the bulk and is, hence, supportive of this model.

#### 4. Concluding Remarks

It is believed that the present work confirms again the importance of higher n-body terms for a correct description of solvated ions, in particular for the case of nonaqueous solvents. The separation of the system into a QM and a MM region does not seem to be a problem for the quality of the results. A further improvement could probably be achieved only by the use of large basis sets and/or inclusion of correlation effects in the QM treatment. This is, however, still beyond any reasonable computational feasibility.

**Acknowledgment.** The access to computing facilities of the High Performance Computing Center at NECTEC is gratefully acknowledged. This project is financially supported by the Thailand Research Fund (Grant No. PDF/24/2541).

#### References and Notes

- (1) Alder, B. J.; Wainwright, T. E. *J. Chem. Phys.* **1957**, *27*, 1208.
- (2) Metropolis, N.; Metropolis, A. W.; Rosenbluth, M. N.; Teller, A. H.; Teller, E. *J. Chem. Phys.* **1953**, *21*, 1087.
- (3) Matsuoka, O.; Clementi, E.; Yoshimine M. *J. Chem. Phys.* **1976**, *64*, 1351.
- (4) Marcus, Y. *Chem. Rev.* **1988**, *88*, 1475.
- (5) Catlow, C. R. A. *Computer Modelling of Fluids Polymers and Solids*; Kluwer Academic Publishers: Dordrecht, The Netherlands 1990.
- (6) Sprik, M. *Computer Simulation in Chemical Physics*; Allen, M. P.; Tildesley, D. J., Eds.; Kluwer Academic Publishers: Amsterdam, 1993; p 211.
- (7) Ortega-Blake, I.; Novaro, O.; Les, A.; Rybak, S. *J. Chem. Phys.* **1982**, *76*, 5405.
- (8) Hannongbua, S.; Kerdcharoen, T.; Rode, B. M. *J. Chem. Phys.* **1992**, *96*, 6945.
- (9) Hannongbua, S. *J. Chem. Phys.* **1997**, *106*, 6076.
- (10) Hannongbua, S. *Chem. Phys. Lett.* **1998**, *288*, 663.
- (11) Warshel, A.; Karplus, M. *J. Am. Chem. Soc.* **1972**, *94*, 5612.
- (12) Field, M. J.; Bash, P. A.; Karplus, M. *J. Comput. Chem.* **1990**, *11*, 700.
- (13) Dunning, T. H., Jr.; Harding, L. B.; Wagner, F. A.; Schatz, G. C.; Bowman, J. M. *Science* **1988**, *240*, 453.
- (14) Bash, P. A.; Field, M. J.; Karplus, M. *J. Am. Chem. Soc.* **1987**, *109*, 8092.
- (15) Gao, J. *J. Am. Chem. Soc.* **1993**, *115*, 2930.
- (16) Kerdcharoen, T.; Liedl, K. R.; Rode, B. M. *Chem. Phys.* **1996**, *211*, 313.
- (17) Tongraar, A.; Liedl, K. R.; Rode, B. M. *Chem. Phys. Lett.* **1998**, *286*, 56.
- (18) Tongraar, A.; Liedl, K. R.; Rode, B. M. *J. Phys. Chem. A* **1998**, *102*, 10340.
- (19) Tongraar, A.; Liedl, K. R.; Rode, B. M. *J. Phys. Chem. A* **1997**, *101*, 6299.
- (20) Hannongbua, S. *Aust. J. Chem.* **1991**, *44*, 447.
- (21) Kerdcharoen, T.; Hannongbua, S. *Chem. Phys. Lett.* **1999**, *310*, 333.
- (22) Marchi, M.; Sprik, M.; Klein, M. L. *J. Phys.: Condens. Matter* **1990**, *2*, 5833.
- (23) Wang, J.; Boyd, R. J.; Laaksonen, A. *J. Chem. Phys.* **1996**, *104*, 7261.
- (24) Kerdcharoen, T. “Hot-Spot” Molecular Dynamics. Ph.D. Thesis, University of Innsbruck, 1995.
- (25) Stevens, W. J.; Basch, H.; Krauss, M. *J. Chem. Phys.* **1984**, *81*, 6026.
- (26) Pulay, P. *Ab initio Methods in Quantum Chemistry II*; Lawley, K. P., Ed.; Wiley: New York, 1987; p 241.
- (27) Brooks, B. R.; Bruccoleri, R. E.; Olafson, B. D.; States, D. J.; Swaminathan, S.; Karplus, M. *J. Comput. Chem.* **1983**, *4*, 187.
- (28) Hannongbua, S.; Ishida, T.; Spohr, E.; Heinzinger, K. *Z. Naturforsch.* **1988**, *43a*, 572.
- (29) Spirko, V. *J. Mol. Spectrosc.* **1983**, *101*, 30.
- (30) Sidhisoradej, W.; Hannongbua, S.; Ruffolo, D. *Z. Naturforsch.* **1998**, *53a*, 208.
- (31) Hannongbua, S.; Rode, B. M. *Chem. Phys.* **1992**, *162*, 257.
- (32) Tongraar, A.; Hannongbua, S.; Rode, B. M. *Chem. Phys.* **1997**, *219*, 279.
- (33) Pranowo, H. D.; Rode, B. M. *J. Phys. Chem. A* **1999**, *103*, 4298.
- (34) Kiselev, M.; Kerdcharoen, T.; Hannongbua, S.; Heinzinger, K. *submitted*.
- (35) Adams, D. J.; Adams, E. H.; Hills, G. J. *Mol. Phys.* **1979**, *38*, 387.

- (36) Marx, D.; Sprik, M.; Parrinello, M. *Chem. Phys. Lett.* **1997**, 273, 360.
- (37) Obst S.; Bradaczek, H. *J. Phys. Chem.* **1996**, 100, 15677.
- (38) Martínez, J. M.; Pappalardo, R. R.; Sanchez Marcos, E.; Refson, K.; Diaz-Moreno, S.; Muñoz-Paez, A. *J. Phys. Chem. B* **1998**, 102, 3272.

- (39) Lee, S. H.; Rasaiah, J. C. *J. Chem. Phys.* **1994**, 101, 6964.
- (40) Caminiti, R.; Licheri, G.; Paschina, G.; Pinna, G. *J. Chem. Phys.* **1980**, 72, 4552.
- (41) Skipper, N. T.; Neilson, G. W. *J. Phys.: Condens. Matter* **1989**, 1, 4141.